J. Membrane Biol. 147, 23–34 (1995)

The Journal of
Membrane
Biology



# Quaternary Ammonium Ion Blockade of $I_K$ in Nerve Axons Revisited. Open Channel Block *vs.* State Independent Block

**J.R. Clay**

Laboratory of Neurophysiology, National Institute of Neurological Disorders and Stroke, National Institutes of Health, Bldg 36, Rm 2C02, Bethesda, Maryland, 20892 and the Marine Biology Laboratory, Woods Hole, Massachusetts, 02543

Received: 7 January 1995/Revised: 26 April 1995

**Abstract.** The mechanism of blockade of the delayed rectifier potassium ion channel in squid giant axons by intracellular quaternary ammonium ions (QA) appears to be remarkably sensitive to the structure of the blocker. TEA, propyltriethyl-ammonium ($C_3$), and propyltetraethylammonium (TAA-$C_3$) all fail to alter the deactivation, or "tail" current time course following membrane depolarization, even with relatively large concentrations of the blockers, whereas butyltriethylammonium ($C_4$), butyltetraethylammonium (TAA-$C_4$), and pentytriethyammonium ($C_5$) clearly do have such an effect. The relative electrical distance of blockade for all of these ions is ~0.25–0.3 from the inner surface of the membrane. The observations concerning TEA, $C_3$, and TAA-$C_3$ suggest that these ions can block the channel in either its open or its closed state. The results with $C_4$, TAA-$C_4$, and $C_5$ are consistent with the open channel block model. Moreover, the sensitivity of block mechanism to the structure of the blocker suggests that the gate is located close to the QA ion binding site and that TEA, $C_3$, and TAA-$C_3$ do not interfere with channel gating, whereas $C_4$, TAA-$C_4$, $C_5$, and ions having a longer hydrophobic "tail" than $C_5$ do have such an effect. The parameters of block obtained for all QA ions investigated were unaffected by changes in the extracellular potassium ion concentration.

**Key words:** Closed channel block — Nerve axon — $K^+$ channel

## Introduction

Potassium ion channels in nerve membranes are blocked in a voltage-dependent manner when tetraethylammonium ions (TEA) are applied on the intracellular side of the membrane in millimolar concentrations. The original reports of this effect in squid giant axons by Armstrong and Binstock (1965) and Armstrong (1966) led to the hypotheses that the channel must open prior to blockade by TEA and that block is antagonized by extracellular potassium ions. These results were amplified by subsequent work with TEA derivatives (Armstrong, 1969; 1971; Armstrong & Hille, 1972; French & Shoukimas, 1981; Swenson, 1981).

A cautionary note regarding the mechanism of TEA blockade was reported by Stanfield (1983) in a seminal review. He observed that open channel block was surprisingly difficult to distinguish from a mechanism in which blockade is independent of channel state. Results reported from this laboratory several years ago with TEA are consistent with this alternative view (Clay, 1985). The experiments in the present study concern some of the TEA derivatives used by Armstrong (1969; 1971) and French and Shoukimas (1981). The surprising conclusion of this work is that the mechanism of blockade of the delayed rectifier potassium ion channel in squid giant axons is remarkably sensitive to the structure of the blocker. Specifically, TEA itself and some of its derivatives are consistent with state-independent block. That is, the closed states of the channel can be blocked equally as well as the open state, whereas other TEA derivatives do appear to require the open channel block model to explain their effects. Tonic or steady-state block was unaffected by changes in the extracellular potassium ion concentration, $K_o$, for all of the quaternary ammonium (QA) ions used in this report. However, an unusual phasic effect of $K_o$ was observed on membrane current waveforms in the presence of QA ion blockade with strong depolarizations.

Some of these results have been reported in abstract form (Clay 1992).

*Correspondence to:* J.R. Clay

## Materials and Methods

Experiments were performed on giant axons from the common North Atlantic squid (*Loligo pealei*) at the Marine Biology Laboratory in Woods Hole, MA using axial wire voltage clamp and intracellular perfusion techniques described in French and Wells (1977) and Clay and Shlesinger (1983). Most experiments were carried out with data acquisition and analysis software implemented on a personal computer (Alembic Software, Montreal, Canada). The temperature in these experiments ranged between 6 and 9°C. In any single experiment it was maintained constant to within 0.1°C by a negative feedback circuit connected to a Peltier device located within the experimental chamber. The extracellular artificial seawater solution in all experiments contained (in mM): 10 $CaCl_2$, 50 $MgCl_2$, 10 Tris-HCl (pH 7.2), 1 μM tetrodotoxin (TTX, Sigma), and either 0, 10, 50, 150, or 300 mM KCl, with, respectively, 440, 430, 390, 290, or 140 mM NaCl. The control intracellular perfusate contained (in mM): 400 sucrose, 25 $K_2HPO_4$, and either 250 K-glutamate, 250 KF, or 200 K-glutamate and 50 KF with the pH adjusted to 7.2. In general, no differences in results were observed with these solutions (Clay, 1988), although the addition of fluoride to the intracellular solution at levels of 50 mM, or higher, clearly does minimize leakage current in midsummer preparations. The blockers employed in this study were added to the control solutions at final concentrations indicated in the text. The blockers used were tetraethylammonium as either the chloride (Sigma), or the iodide salt (Eastman Kodak); propyl-, butyl-, pentyl-, and nonyltriethylammonium as the iodide salts (Cambridge Chemical, Milwaukee, WI); and propyl- and butyl-tetraethylammonium as the chloride salts (Eastman). The $C_n$ nomenclature used below, where n is either 3, 4, 5, or 9, refers to the triethylammonium ion derivatives, propyl-, butyl-, pentyl-, or nonyltriethylammonium, respectively. The number of carbon atoms in each of the side chains of the symmetric tetraalkylammonium (TAA) ion compounds propyl- and butyl-tetraethylammonium (3 and 4, respectively) is referred to on the abscissa of Fig. 9. TEA itself, which is referred to as $C_2$ below, can be thought of as belonging to either the TAA or the triethylammonium ion series.

The fits of the Woodhull (1973) model (illustrated in the lower right insert of Fig. 8) to the QA block results in Figs. 8–10 were obtained by least squares minimization.

## Results

### Blockade with Single Depolarizing Voltage Clamp Steps

The effects of $C_2$, $C_3$, $C_4$, and $C_5$ on outward delayed rectifier current, $I_K$, during a depolarizing voltage step (+100 mV) are illustrated in Fig. 1*A–D*, respectively, for four different axons in control conditions and with the concentration of each blocker as indicated. The test records in Fig. 1 illustrate the familiar time-dependent "inactivation" effect (Armstrong, 1969; 1971). That is, $I_K$ in the presence of these quaternary ammonium (QA) ions appears to activate and then "inactivate" as though the channels must open before blockade can occur. However, these results do not conclusively confirm this mechanism, as Armstrong (1969) and Stanfield (1983) have noted. Stanfield (1983) in particular observed that a parallel, or state independent blocking mechanism could equally well describe results such as those in Fig. 1. That is, the "inactivation" feature could reflect the time- and voltage-dependent interaction of a QA ion with its binding site within the electric field of the channel. This point is illustrated in Fig. 2 in which the open channel and state independent block models are described. The channel state descriptions of each model are shown below Fig. 2*C* and 2*D*, respectively. The [C] ··· [C] feature in both models represents the series of closed states through which the channel is believed to pass following membrane depolarization, before opening occurs. This mechanism describes the sigmoidal, time-dependent activation of $I_K$ in control (Hodgkin and Huxley, 1952; Fitzhugh, 1965). The channel must open before blockade can occur in the model described below Fig. 2*C*, whereas blockade can proceed from any state of the channel in the model described below Fig. 2*D*, as indicated by states [CB] and [OB], which refer to closed and blocked, or open and blocked, respectively. The prediction of each model for depolarizing steps in control and in the presence of a QA blocker are illustrated in Fig. 2*A* and *B*, respectively, for parameters of the various rate constants as given in the legend of Fig. 2. The control waveforms are, of course, the same in each model. The test waveforms are surprisingly similar, which indicates that results such as those in Fig. 1 cannot conclusively distinguish between these models. This conclusion is independent of the model of channel activation used in the simulation. Clearly, variations of the blocking mechanisms illustrated in Fig. 2 could also be taken into consideration. This study focuses on the two models described in the bottom panels of Fig. 2, because a physical mechanism for each for QA blockade can be clearly envisioned (Discussion).

### Tail Currents

As Stanfield (1983) noted, a clear difference in the predictions of the models described in Fig. 2 concerns deactivation, or "tail current" results. A corollary to the idea that the channel must open before blockade can occur is that the blocker must leave the channel before the channel can close. Consequently, the tail current time course is effectively slowed, whereas no such effect occurs with state independent block. The analysis is simplified by the observation that the forward rate constant for channel activation, $\alpha$, in Fig. 2, for potentials negative to rest is essentially nil. Consequently, the tail current time constant, $\tau$, for the open channel block model in the presence of the blocker is approximately given by $\beta^{-1}\lambda^{-1}(\lambda + \kappa)$ when $\lambda$ and $\kappa$ are $\gg$ than $\beta$, which appears to be the case for the blockers used in this study, whereas $\tau$ is given by $\beta^{-1}$ for state-independent block regardless of whether or not the blocker is present (Clay, 1985). The forward rate constant for blockade, $\kappa$, is a

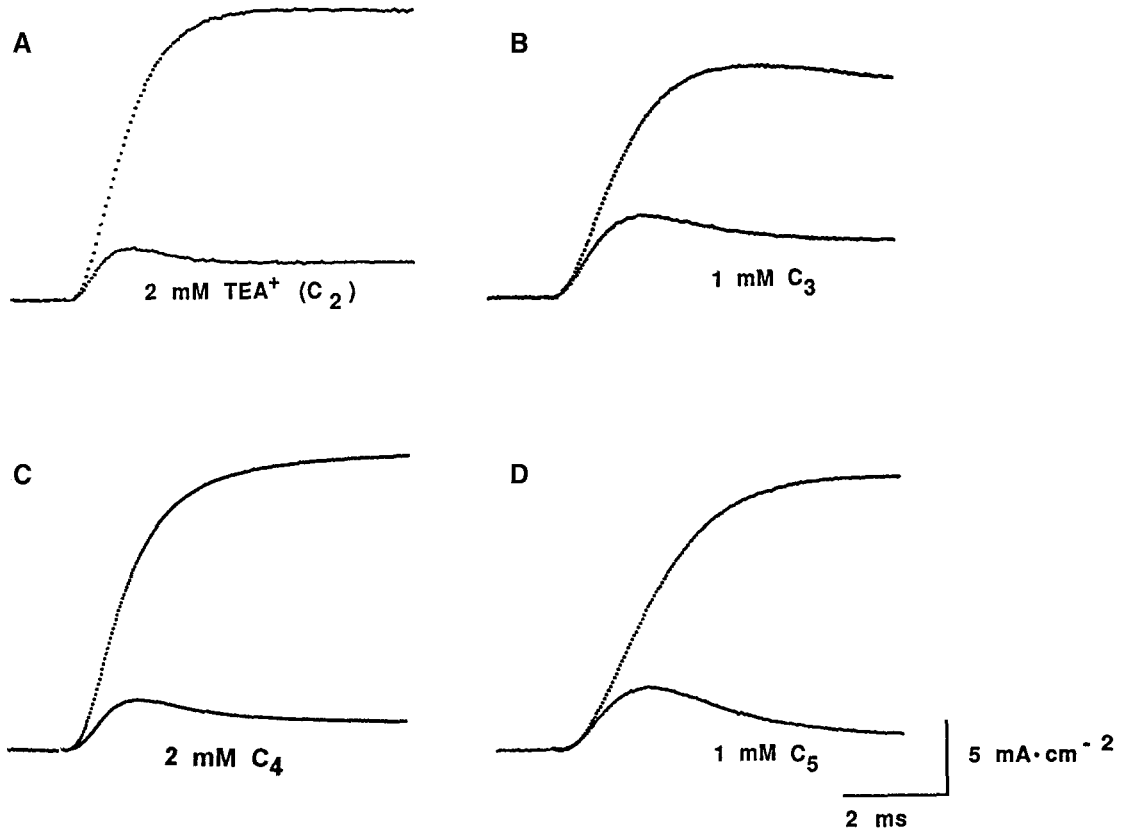


**Fig. 1.** Effects of triethylammonium ion derivatives on outward current. In each panel the membrane potential was stepped to +100 mV from a holding potential of −80 mV in control and five min after the addition to the intracellular perfusate of each respective blocking ion at the concentration indicated. The control and test records are superimposed. Each panel is taken from a different axon. Records leak current corrected. External solution contained 10 mM $K_o$ in each case.

pseudo-first order rate parameter, since it depends upon the concentration of the blocker [QA], i.e., $\kappa = \kappa_1[QA]$, so that $\tau$ in the open channel block model is given by $\tau = \beta^{-1}(1 + \kappa_1[QA]\lambda^{-1})$. That is, $(\tau/\tau_o - 1)$, where $\tau_o$ is the time constant in control, is predicted to linearly increase with concentration of the blocker in the open channel block model. Outward current is predominantly blocked by intracellular QA ions, although inward current is also blocked, provided the concentration of the blocker is sufficiently large (Blatz & Magleby, 1984). The predictions of the two models for conditions in which approximately 50% of inward current is blocked following activation of the conductance by a depolarizing prepulse are illustrated in Fig. 2*C* and *D*, respectively. Both models show a "hook" in the tail currents, as originally observed by Armstrong and Binstock (1965), which reflects a rapid unblocking of the channel. That is, the steady state block at the potential corresponding to the tail current is significantly less than that at the end of the depolarizing prepulse. Consequently, some channels are unblocked immediately following a subsequent hyperpolarizing step thereby leading to a rapid increase of conductance. The current then relaxes to zero as channels close. Moreover, the closing process is slowed in the open channel block model, whereas it is unaffected in the state independent block model. Tail current results with TEA ($C_2$) are consistent with state-independent block, as previously shown (Clay, 1985). A similar result is illustrated in Fig. 3*A* for 25 mM TEA. In this experiment, the membrane potential was stepped to 0 mV from a holding potential of −80 mV with 300 $K_o$ (300 $K_i$) to activate the conductance without producing significant net current. The membrane potential was then stepped back to −120 mV. Approximately 70% of the conductance was blocked at this potential. However, the tail current time constant was not significantly altered. This result was independent of TEA concentration, as shown by the results in Fig. 3*B* for 2 and 50 mM TEA from a different preparation. Further results of this nature from two other preparations are shown in Fig. 4 for 10 mM TEA with test potentials of −80, −100 and −120 mV, which demonstrate that the lack of effect of TEA on the tail current time constant is independent of membrane potential. The lack of effect of TEA on tail current time constant was also independent of changes in external potassium ion concentration (*results not shown*).

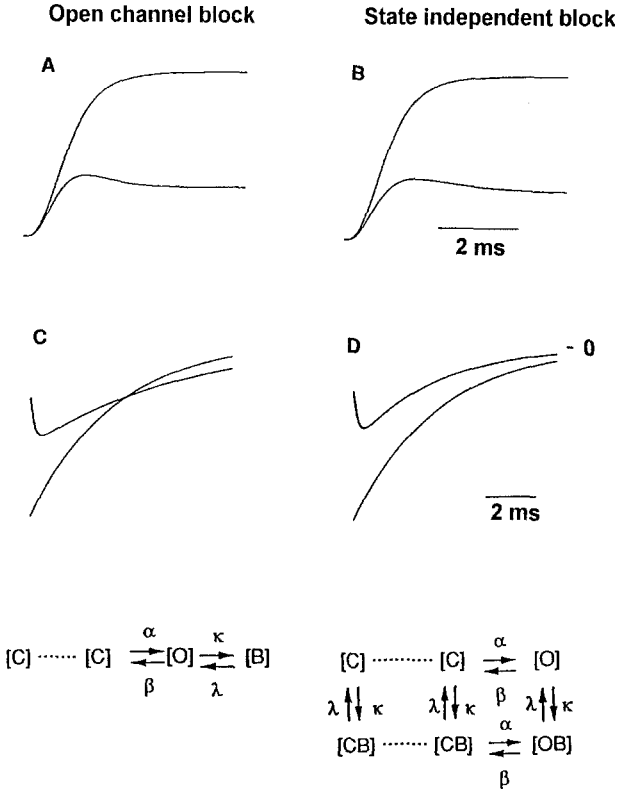


**Fig. 2.** Theoretical predictions of the open channel and state independent block models are described in the text. (*A*) The control trace represents the open state probability in the Hodgkin and Huxley (1952) model for the delayed rectifier at strongly depolarized potentials. This curve is given by $(1 - \exp(-t/\tau))^4$, where $\tau = 0.67$ msec. The test trace corresponds to QA blockade with the open channel block mechanism. This curve was calculated from the Markov chain representation (Fitzhugh, 1965) of the Hodgkin and Huxley (1952) model given by

$$[C] \underset{\beta}{\overset{4\alpha}{\rightleftharpoons}} [C] \underset{2\beta}{\overset{3\alpha}{\rightleftharpoons}} [C] \underset{3\beta}{\overset{2\alpha}{\rightleftharpoons}} [C] \underset{4\beta}{\overset{\alpha}{\rightleftharpoons}} [O] \underset{\lambda}{\overset{\kappa}{\rightleftharpoons}} [B]$$

with $\alpha = 1.5$ msec$^{-1}$, $\beta = 0$, $\kappa = 1.4$ msec$^{-1}$, and $\lambda = 0.6$ msec$^{-1}$, [This description of the model also gives $(1 - \exp(-t/\tau))^4$ for the open state probability with $\kappa = 0$]. (*B*) Same control as in *A*. The test trace represents the prediction of state independent block, which is given by $(1 - \exp(-t/\tau))^4(p_{NB} + (1 - p_{NB})\exp(-t/\tau_B))$, where $\tau = 0.67$ msec, $\tau_B = (\kappa + \lambda)^{-1} = 1.5$ msec, and $p_{NB}$, the probability that the channel is not blocked in the steady state, is 0.3. [The vertical scale, which is arbitrary, is the same as in *A*.] (C) Tail current at strongly hyperpolarized potentials in control and in the open channel block model. The control represents $-\exp(-t/\tau)$ with $\tau = 2.1$ msec. The test curve represents $a \exp(-(\kappa + \lambda)t) + b \exp(-\lambda t(\kappa + \lambda)\tau))$, where $\kappa = 3.1$ msec$^{-1}$, $\lambda = 4.02$ msec$^{-1}$, $\tau = 2.1$ msec, $a = 0.3$, and $b = -0.56$. (*D*) Same control curve as in *C*. The test curve is the prediction of the state independent model for tail current, which is given by $\exp(-t/\tau)[a \exp(-(\kappa + \lambda)t) + b]$, with *a, b,* $\tau$, $\kappa$, and $\lambda$ as given in *C*. The vertical scale is the same as in *C*.

The question that arises from the results in Figs. 3 and 4 with TEA is what are the effects of other blockers on tail currents, especially considering the compelling evidence for the open channel block model provided by Armstrong (1969) for $C_5$. This issue is addressed by the results in Fig. 5 in which tail current results are illustrated for $C_2$ (TEA), $C_3$, $C_4$, and $C_5$ with a concentration of 10 mM for $C_2$, $C_3$, and $C_4$, and 1.2 mM for $C_5$. The degree of block is approximately the same for all four experiments, which indicates that $C_5$ is a significantly more potent blocker than the other three ions, as further shown in Fig. 9. Moreover, the tail current time constant for $C_3$ (Fig. 5*B*) is unaltered as shown again in Fig. 5*A* for TEA ($C_2$). By contrast, the tail current in the presence of the blocker "crosses-over" the corresponding control result for $C_4$ and $C_5$ (Fig. 5*C* and *D*, respectively), as well as for $C_9$ (*results not shown*) in a manner which is consistent with open channel block. In other words, the addition of a *single* carbon atom to the *n*-terminus of $C_3$ is sufficient to modify the mechanism of blockade from state independent ($C_3$) to state dependent ($C_4$), that is, open channel blockade. As noted above, $(\tau/\tau_o - 1)$, where $\tau_o$ is the tail current time constant in control, is predicted to increase at any given potential with the concentration of the blocker if blockade occurs only in the open state, as appears to be the case with $C_4$. The results in Fig. 6 from three different preparations with either 2 or 10 mM $C_4$ are consistent with this prediction.

Results similar to those for the $C_n$ ions concerning the transition in mechanism of blockade from state independent to open channel block when the number of carbon atoms on the *n*-terminus was raised from 3 to 4 were also observed with TAA ions, as shown in Fig. 7. Specifically, propyltetraethylammonium (TAA-$C_3$) did not alter the tail current time constant (Fig. 7A) as with the results with $C_3$ in Fig. 5*B*, whereas butyltetraethylammonium (TAA-$C_4$) did have such an effect (Fig. 7*B*) similar to that of $C_4$, as shown in Fig. 5*C* and Fig. 6*C–D*. The implications of these results for channel structure are given below (Discussion).

## Quantitative Analysis of the Voltage Dependence of Blockade

The voltage dependence of QA blockade of the potassium ion channel can be described with Eyring rate theory in a manner similar to that originally used by Woodhull (1973) to describe blockade of the sodium channel by hydrogen ions. The model is illustrated in the lower right hand inset of Fig. 8. As noted above, the forward rate constant of blockade, $\kappa$, is given by $\kappa = \kappa_1[QA]$. The parameter $\kappa_1$ is, in turn, given by $\kappa_o \exp(d_1 qV/kT)$ where $d_1$ is the electrical distance which the blocker must cross to reach its binding site within the channel, and *q*, *k*, and *T* all have their usual meanings, with $kT/q \sim 24$ mV at 8°C. The reverse rate parameter, $\lambda$, is given by $\lambda = \lambda_o \exp(-d_2 qV/kT)$. (The line labeled $\infty$ in Fig. 8 indicates that these blockers are unable to pass through the

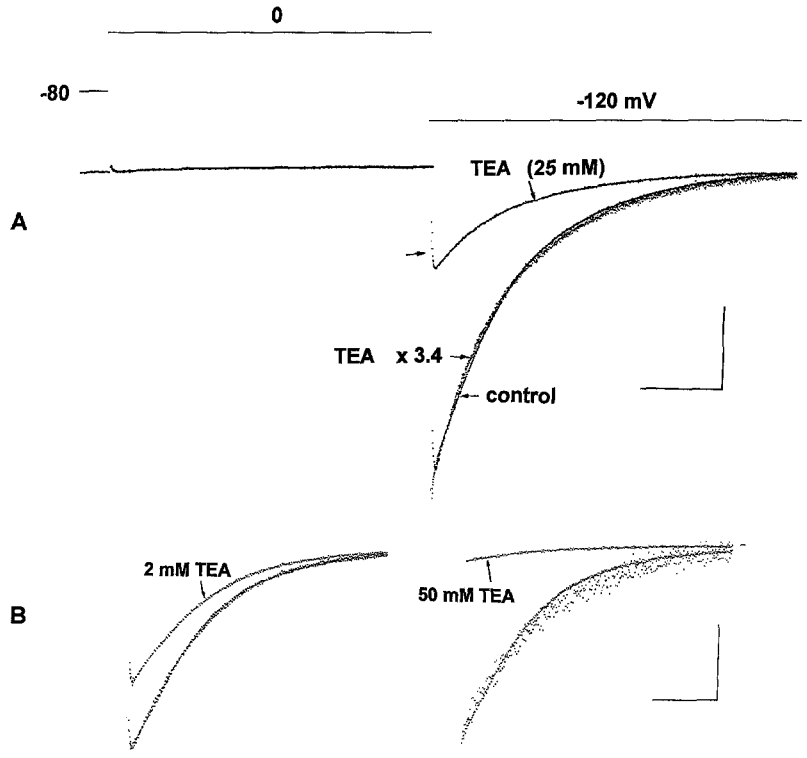


**Fig. 3.** Lack of effect of TEA on tail current time course. (*A*) In this experiment, the membrane potential was stepped to 0 mV for 20 msec in control (300 $K_i$, 300 $K_o$) and with 25 mM TEA in the intracellular perfusate followed by a step back to −120 mV. The control and test records are superimposed. The test tail current is also shown scaled by a factor of 3.4. The responses elicited by the step to 0 mV have been leak corrected. The tail currents are uncorrected, save for the scaling procedure. The arrow near the initial portion of the test record indicates the "hook" in the test result described in the text. Calibrations: 5 msec and 5 mA·cm$^{-2}$. *B* Lack of effect of two different concentrations of TEA (2 and 50 mM) on tail current time constant. Same conditions as in *A* with a test potential of −100 mV. In each case, the TEA result is also shown scaled so as to closely match the control result. The scaling factor was 1.45 and 11.0 for the 2 and 50 mM TEA results, respectively. Calibrations are 5 msec and 2 mA · cm$^{-2}$. Different preparation than in *A*.

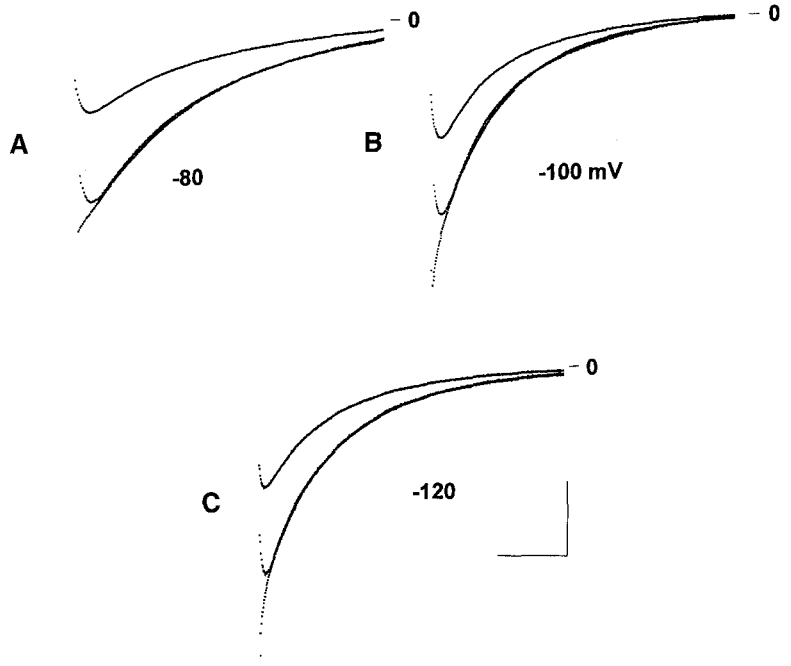


**Fig. 4.** Lack of effect of $TEA^+$(10 mM) on tail current time constant at various different test potentials. Same experimental conditions as for the result in Fig. 3. Results in *A* and *B* for −80 and −100 mV, respectively, were taken from a single preparation. The result in *C* for −120 mV was taken from another axon. The test record in each case is shown scaled by a factor equal to 2.1, 1.7, and 1.8 for *A*, *B*, and *C*, respectively. Horizontal scale is 5 msec. Vertical scale is 3 mA · cm$^{-2}$.

channel.) The fraction of unblocked channels in the steady state is given by $(1 + [QA]K_D^{-1}\exp(dqV/kT))^{-1}$, where $K_D$, the dissociation constant at 0 mV, is equal to $\lambda_o/\kappa_o$, and $d = d_1 + d_2$. The parameters $d$ and $K_D$ can be obtained from a fit to the steady-state current voltage relation in the presence of the blocker, as illustrated in Fig. 8. The control results in this experiment (●) were obtained from the instantaneous *I-V* relation following a 15 msec prepulse to 0 mV to activate the conductance followed by steps to the potentials indicated on the abscissa of Fig. 8. These results are well described by a straight line. The test results for steady state blockade at depolarized potentials were obtained in most experiments from the steady-state current, as with the results in

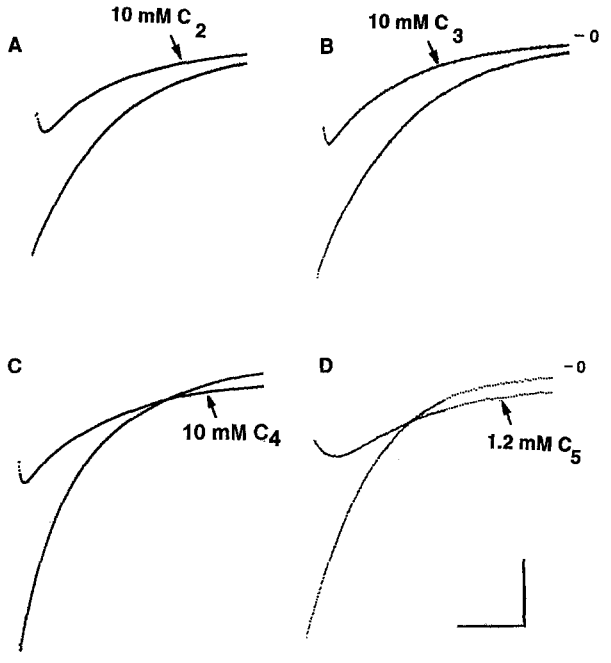


**Fig. 5.** Effects of triethylammonium ion derivatives on tail current kinetics. The concentration of each $C_n$ derivative in the intracellular perfusate is indicated in each panel. In particular the concentration used for $C_2$, $C_3$, and $C_4$ was 10 mM, whereas 1.2 mM was used for $C_5$. The ionic conditions were the same as in Figs. 3 & 4 (300 $K_i$; 300 $K_o$). The membrane potential was stepped to 0 mV for 20 msec both in control and in test conditions followed by a step to −80 (*A*), −100 (*B*), −100 (*C*), or −90 mV(*D*). The control and test results are superimposed in each panel. Each panel illustrates results from a different axon. The horizontal calibration represents 4.0, 3.5, 4.5, or 5 msec for *A*, *B*, *C*, or *D*, respectively. The vertical calibration represents 2.5, 1.0, 2.5, or 2.3 mA · $cm^{-2}$ for the same respective sequence.

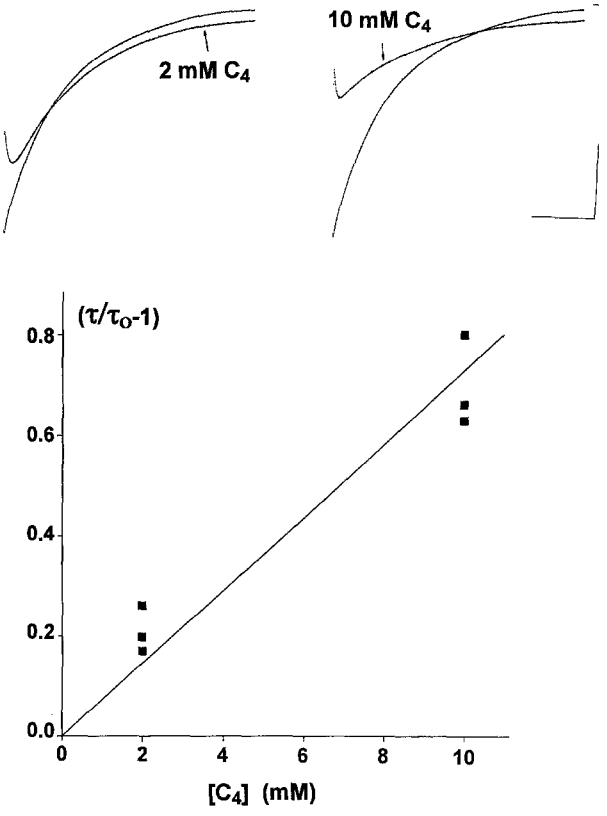


**Fig. 6.** Concentration dependence of tail current time constant with $C_4$. The records shown in the top part of the figure correspond to 2 and 10 mM $C_4$, as indicated. Same experimental protocol as in Fig. 3. Test potential was −100 mV. Calibrations are 2.5 mA · $cm^{-2}$ and 5 msec. The bottom part of the figure illustrates ($\tau/\tau_o$ − 1), where $\tau$ and $\tau_o$ are the tail current time constants in the presence of blockade and in control, respectively. The symbols were taken from three different preparations with a test potential of −100 mV in each case.

Fig. 10, or, as in the results in Fig. 8, from the point where blockade reached its steady state level appropriate to the test potential (indicated by the line labeled *a* in the inset of Fig. 8), but before the slight additional activation of conductance that occurred in this experiment during the test step. The steady-state blockade at hyperpolarized potentials cannot be as readily obtained as with depolarizing pulses, since the channels are closed in the steady state for these conditions, and the removal of block which occurs at these potentials (the "hook" in the tails) does not take place instantaneously. This result can be determined from the extrapolation of the tail current to the beginning of the test step, as indicated, for example, by the arrow labeled *b* alongside the −100 mV record in Fig. 8.

The current-voltage relations obtained as described above were fit to the relation $g_K(V - E_K)/(1 + [QA]K_D^{-1}\exp(dqV/kT))$, as shown in Fig. 8, where $g_K$ and $E_K$ were obtained from the control *I-V*, and $K_D$ and $d$ were obtained from the test results. A summary of results for $d$ and $K_D$ for the blockers used in this study are shown in Fig. 9, top two panels, respectively. The solid symbols (●) in Fig. 9 refer to the triethylammonium ion derivatives, $C_n$, where n is given on the abscissa. The open symbols (○) refer to the TAA ions, where n = 3 indicates propyltetraethylammonium (TAA-$C_3$) and n = 4 indicates butyltetraethylammonium (TAA-$C_4$). The results in the top panel of Fig. 9 indicate that all of these ions have a common electrical distance, $d = d_1 + d_2$, for their binding site within the channel, where $d \sim 0.25$–$0.3$ from the inner surface of the membrane. The results in the middle panel indicate that potency of block with $C_n$ increases with increasing n, as was noted originally by Armstrong (1969). These results indicate a rather striking dependence of $K_D$ on the length of the *n*-terminus. The $K_D$ for $C_2$, $C_3$, and $C_4$ decreases only slightly with increasing n, whereas a marked increase of potency occurs beginning with $C_5$, as shown by the block of tail currents in Fig. 5. Similar results were recently obtained for the *Shaker* potassium channel by Choi, et al. (1993).

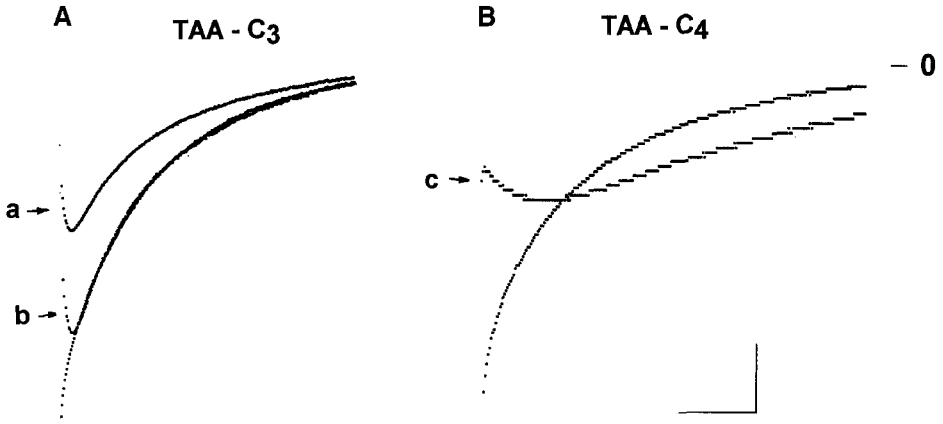


**Fig. 7.** Block of tail currents by the tetraalkylammonium ion derivatives propyltetraethylammonium (TAA-$C_3$) and butyltetraethylammonium (TAA-$C_4$). Same experimental conditions as in Figs. 3 with 50 mM TAA-$C_3$ added to the intracellular perfusate in *A* and 0.25 mM TAA-$C_4$ added to the intracellular perfusate in *B*. The test potential for the results in both *A* and *B* was −120 mV. The test result is labeled *a* in the left hand panel. The result labeled *b* corresponds to the test record scaled by a factor of 1.65. The record labeled *c* in the right hand panel is the test record scale by a factor of 1.5. Horizontal calibration corresponds to 1.5 msec in *A* and 2 msec in *B*. Vertical calibration corresponds to 2 mA · $cm^{-2}$ for both *A* and *B*.

They also found relatively little difference in blockade amongst $C_2$, $C_3$, and $C_4$, whereas $C_n$ with $n \geqslant 6$ caused a marked increase in potency.

The results with the TAA ions are quite different from the $C_n$ results, a finding which is original to this study. In particular, TAA-$C_3$ is almost 10-fold less potent than propyltriethylammonium ($C_3$), whereas TAA-$C_4$ is 10-fold more potent than butyltriethylammonium ($C_4$). The relative potency of the blockers does not appear to be related to the mechanism of blockade, since $C_4$ is only slightly more potent than $C_3$, (Figs. 5 and 9), whereas TAA-$C_4$ is substantially more potent than TAA-$C_3$, and the transition in block mechanism occurs between $C_3$ and $C_4$, as well as between TAA-$C_3$ and TAA-$C_4$. The key point concerning mechanism of block appears to be the number of carbon atoms on the side groups of these ions.

The analysis given above for the parameters of steady-state blockade depends upon *d*, the distance from the inner membrane surface to the QA ion blocking site. The kinetics of block depend upon $d_1$, the electrical distance of the barrier which these ions must cross to reach the blocking site. The forward rate constant for blockade, $\kappa$, is clearly voltage dependent, whereas the voltage dependence of the reverse parameter, $\lambda$, is less clear. Two possibilities for this aspect of the model are illustrated by the barrier diagrams in Fig. 10. The diagram on the left corresponds to a lack of voltage dependence for $\lambda$, i.e., $d_2 = 0$, or $d_1 = d$. A second possibility, shown by the diagram on the right of Fig. 10 corresponds to $d_1 = d_2$. The block kinetics in either case are given by $\tau = (\lambda + \kappa)^{-1} = (\lambda_o \exp(-d_2 qV/kT) + \kappa_o[QA]\exp(d_1 qV/kT))^{-1}$. Values of $\tau$ obtained from the results in Fig. 10 with 10 mM TEA are indicated by the symbols (●). The time constant decreases only slightly with depolarizations positive to $V = 0$ mV for these conditions. Moreover, $\tau$ is also relatively independent of potential for $V < 0$ mV (the "hooks" in the tail currents). Overall these results are consistent with a barrier model in which $d_1 \sim d_2$. A model in which $d_2 = 0$, i.e., a lack of voltage dependence for $\lambda$, predicts too great a voltage dependence for $\tau$. The seemingly paradoxical conclusion from this analysis is that the relative lack of voltage dependence for $\tau$, especially for tail currents, argues in favor of a significant voltage dependence for $\lambda$.

The results for $\lambda_o$ with $d_1 = d_2$ for the various blockers used in this study are shown in the bottom panel of Fig. 9. This analysis indicates that the changes in $K_D$ with QA ion structure noted in the middle panel of Fig. 9 are due in approximately equal measure to changes in both $\lambda_o$ and $\kappa_o (K_D = \lambda_o/\kappa_o)$. For example, $C_9$ is 30-fold more potent than $C_2$, whereas $\lambda_o$ for $C_9$ is about 6-fold less than it is for $C_2$, which indicates that $\kappa_o$ is 5-fold larger for $C_9$ than it is for $C_2$.

### Effects of Extracellular Potassium Ions

An increase in the extracellular potassium ion concentration, $K_o$, produces little effect on outward current in the presence of intracellular TEA, whereas inward current is significantly increased, as originally demonstrated by Armstrong and Binstock (1965). These results might suggest that TEA is swept out of the channel by an increase in $K_o$, i.e., the "knock-off" effect, except that a similar result occurs in control due to the outward rectification of the current-voltage relation of the delayed rectifier channel. This result is shown in Fig. 11 and in

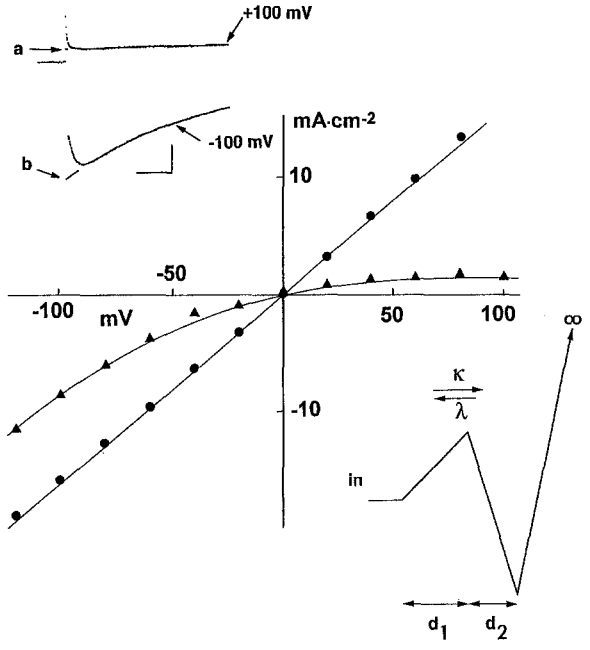


**Fig. 8.** Procedure used to determine the parameters of steady state block by QA ions. These are: $d$ ($d = d_1 + d_2$), the electrical distance of blockade from the inner surface of the membrane, as indicated in the lower right hand inset; and $K_D$, the dissociation constant at 0 mV. The upper left inset illustrates records obtained with 10 mM TEA at +100 and −100 mV following a 15 msec step to 0 mV with 300 $K_i$ and 300 $K_o$. The arrow labeled *a* represents the current after block had reached steady state. The arrow labeled *b* represents the extrapolation of the tail current at −100 mV to the beginning of the test step. This procedure was used to obtain steady state blockade at hyperpolarized potentials, as described in the text. Calibrations are 2 msec and 2 mA · $mA^{-2}$. The symbols (●) are the control instantaneous *I-V* results which were fit by least squares minimization by a straight line having a slope, $g_K$, of 168 mA · $cm^{-2}$. The symbols labeled (▲) are the steady state results in the presence of the blocker. The curve is a fit of these results by $g_K V/(1 + [TEA^+]K_D^{-1}\exp(dqV/kT))$, where $[TEA^+]$ is 10 mM, $kT/q = 24$ mV, and the best fit values of $K_D$ and d are 3.3 mM and 0.26, respectively.

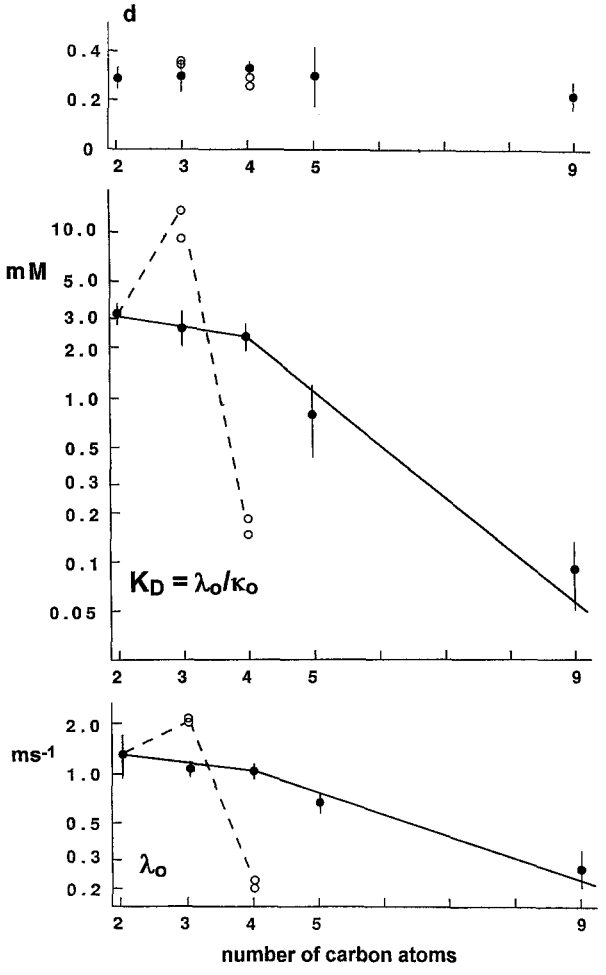


**Fig. 9.** Dependence of QA block parameters $d$, $K_D$, and $\lambda_o$ on structure of the blocker. The symbols (●) represent the triethylammonium ions, $C_n$, where n is given on the abscissa. These are the averaged results from 4 different preparations for each compound. The error bars represent ± SD. The symbols (○) represent tetrapropylammonium (n = 3) and tetrebutylammonium (n = 4). Two experiments for each of these blockers. The lines were drawn by eye.

previous reports (Clay & Shlesinger, 1983; Clay, 1991). That is, the instantaneous *I-V* relation has a nonlinear dependence upon driving force, $(V - E_K)$ when $K_o \neq K_i$, where $E_K$ is the potassium ion equilibrium potential, which is well described by the Goldman, Hodgkin, and Katz, or GHK equation (Goldman, 1943; Hodgkin and Katz, 1949), i.e., $I_K \sim V(\exp(q(V - E_K)/kT) - 1/(\exp(qV/kT) - 1)$. Consequently, the significant increase in tail current amplitude in the presence of TEA produced by an increase in $K_o$ appears not to be related to an interaction between TEA and potassium ions in the channel. This point is further demonstrated by the current-voltage relations in Fig. 11 with either 50 or 300 $K_o$ in control and 6 mM TEA in the intracellular perfusate for either level of $K_o$. The theoretical lines are a best fit description of these results by the GHK equation factored by $(1 + [TEA]K_D^{-1}\exp(dqV/kT))^{-1}$, with [TEA] equal to either 0 or 6 mM. Approximately the same values of $d$ and $K_D$ were obtained from this analysis for either level of $K_o$.

A lack of effect of $K_o$ on block parameters was also observed with the other $C_n$ ions used in this report, as illustrated in Fig. 12 for $C_3$ and $C_4$ (1 mM in each case, steps to +90 mV). In particular, the steady-state current at the end of these voltage steps was the same in either 0 or 150 mM $K_o$, similar to the results with TEA itself, shown in Fig. 11. (The steady-state current in the presence of blockade was also unaffected by a previous depolarizing pulse.) A clear effect of $K_o$ was observed on the peak outward current elicited by the voltage step, an effect which has not been previously reported. The difficulties in interpreting this result are noted below.

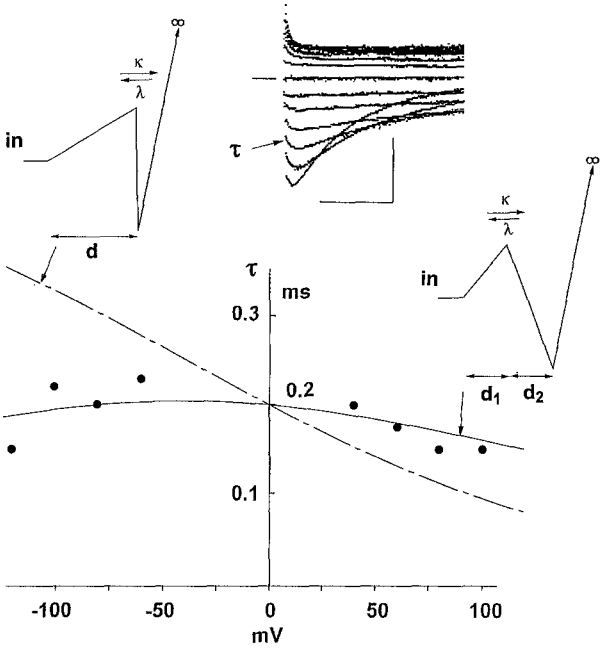


**Fig. 10.** Kinetics of QA blockade. The inset illustrates records obtained by a 15 msec prepulse to 0 mV (300 $K_i$; 300 $K_o$; 5 mM $TEA^+$) and test steps to +100, 80, . . ., −120 mV. Calibrations are 2 msec and 4 mA · $cm^{-2}$. The symbols (●) are best fits to the time constants of block (and unblock), τ, obtained by a single exponential fit ($V > 0$) and a double exponential fit ($V < 0$; i.e., the "hooks" in the tail currents). The broken curve is the prediction of the barrier model illustrated in the upper left inset in which the voltage dependence is ascribed entirely to the forward rate constant, κ. The continuous curve is the prediction of the barrier model illustrated in the upper right inset with $d_1 = d_2$. In both cases $d = 0.25$, $\kappa_o = 0.2$ $msec^{-1} \cdot mM^{-1}$, and $\lambda_o = 2$ $msec^{-1}$.

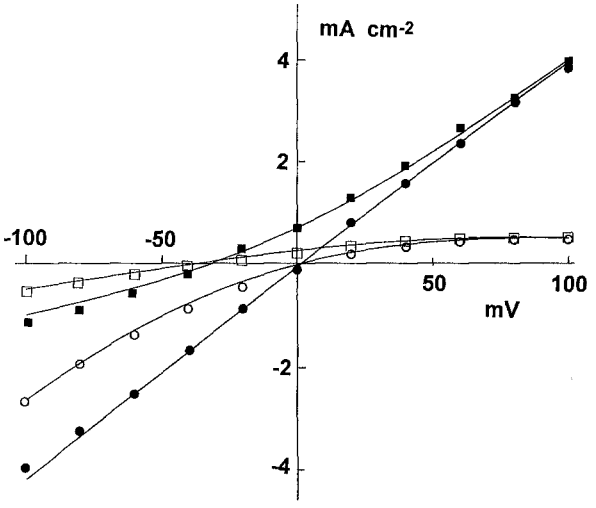


**Fig. 11.** Lack of effect of an increase in extracellular potassium ion concentration, $K_o$, on TEA blockade. The current-voltage relations were obtained following a 15 msec prepulse to 0 mV with either 50 (■), or 300 $K_o$ (●), and with 6 mM TEA in the intracellular perfusate with either 50 (□) or 300 $K_o$ (○). The theoretical lines are best fits to these results of the relation $V(K_i \exp(qV/kT) - K_o)/(\exp(qV/kT) - 1)(1 + [TEA]K_D^{-1}\exp(dqV/kT))^{-1}$, where $kT/q = 24$ mV, $K_i = 290$ mM, [TEA] = either 0 or 6 mM, and $K_o = 300$ mM for the 300 $K_o$ results either in control or with 6 mM TEA, or $K_o = 75$ mM for 0 TEA and 50 $K_o$ or $K_o = 60$ mM for the 6 mM TEA and 50 $K_o$. The differences between $K_o$ used in the equation and the potassium ion concentration in the external medium with 50 mM $K_o$ are attributable to potassium ion accumulation during the prepulse to 0 mV. The best fit values obtained for $K_D$ and $d$ from this analysis for TEA block were $K_D = 3.2$ or 3.4, and $d = 0.33$ or 0.34 for 300 $K_o$ and 50 $K_o$, respectively.

## Discussion

The primary result in this study is the demonstration of an exquisite sensitivity of the mechanism of blockade of axonal potassium channels to the structure of quaternary ammonium ions. Specifically, the addition of a single carbon atom to the *n*-terminus of $C_3$ alters the mechanism of blockade from state-independent ($C_3$) to open channel block ($C_4$). A similar transition occurs between tetrapropylethylammonium and tetrabutylethylammonium. Observations comparable to these results have not been previously reported.

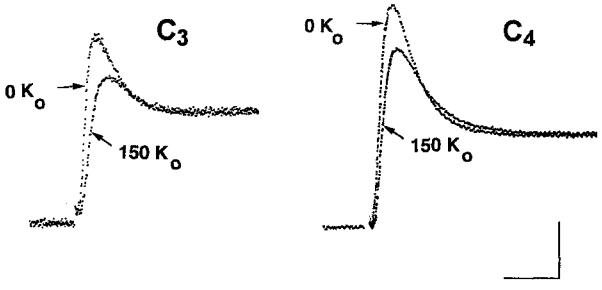


**Fig. 12.** Effect of an increase of $K_o$ on membrane current waveforms with strong depolarization for $C_3$ and $C_4$ (1 mM in each case). Step potential was +90 mV in each case. Results shown superimposed for 0 and 150 mM $K_o$. Calibrations are 2 msec and 0.5 mA · $cm^{-2}$.

### Physical Model of QA Blockade

The effects of QA ions are suggestive of the model of the ion channel-QA ion interaction illustrated in Fig. 13. The internal mouth, or vestibule of the channel, is believed to be relatively wide since TEA is able to enter the channel from the inside and bind at some distance within the electric field of the membrane (Armstrong, 1975). The gating process in the model is postulated to lie, at least in part, near the narrowest part of the vestibule close to the binding site for TEA and the other QA derivatives. The observation that neither TEA, $C_3$, nor TAA-$C_3$ alters tail current kinetics suggests that the binding site for the charge on the head group of these ions lies slightly away

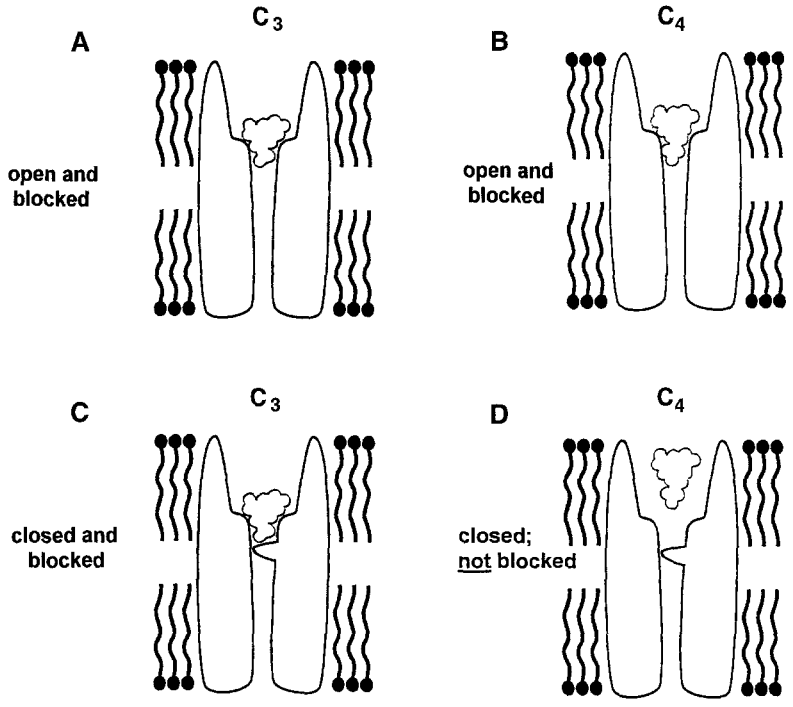


**Fig. 13.** A model of QA ion interaction with the potassium channel as described in the text. The vestibule facing the intracellular side of the membrane is shown along with Corey-Pauling-Koltun silhouettes of $C_3$ (*A* and *C*) and $C_4$ (*B* and *D*). $C_3$ can block either the closed or the open state of the channel. Blockade by $C_4$ requires that the channel be opened first by membrane depolarization.

from the gate towards the intracellular surface of the membrane. That is, these ions can reside at the QA binding site independent of whether or not the gate is open (state independent blockade), as illustrated in Fig. 13*A* and *C*, respectively. The energetically favored orientation of a $C_n$ ion within the channel with $n \geqslant 3$ probably corresponds to the hydrophobic tail of the blocker pointing away from the intracellular medium towards the permeation pathway. The observation that $C_4$, TAA-$C_4$, and $C_n$ with $n > 4$ alter the tail current time constant suggests that the *n*-terminal group of the $C_n$ ion cannot enter the permeation pathway thereby allowing both the head group and the hydrophobic tail to reach their respective binding sites, unless the gate is open (Fig. 13*D*). In other words, the effects of these ions are consistent with the open channel block model. This sensitivity of blockade mechanism to the structure of the QA ion suggests that the blocking site lies only a few Å from the channel gate. A corollary to this observation is that only 70–75% of the electrical potential drop across the channel influences gating, given that the electrical distance of blockade for TEA and its derivatives is 0.25–0.30.

The model in Fig. 13 is to be contrasted with the model proposed by Armstrong (1975; 1990). He places the gate on the inner surface of the membrane at the entrance of the vestibule. In other words the gate must open before blockade can occur with any of the QA ions, which is at odds with the results in this study. Nevertheless, TEA itself does appear to require the open channel block model for other types of $K^+$ channels, as noted below. The question that arises from this observation is how can the model in Fig. 13 conceivably be consistent with the results from other channels given that the region of the channel in which the QA binding site is located appears to be well conserved amongst the various different types of $K^+$ channels (Yellen, et al., 1991; Hartmann, et al., 1991). The answer to this question may lie in the remarkable sensitivity of blockade mechanism to the structure of the blocker demonstrated in this report. $C_4$ and blockers having a longer hydrophobic tail do require the open channel block model for the squid axon $I_K$ channel. $C_2$ and $C_3$ do not. However, a very slight change in the location of the binding site for the charge on the head group of these ions by no more than a few Å in the squid axon channel away from the inner surface of the membrane would appear to be sufficient to require the channel gate to open for TEA blockade to occur. In other words, perhaps only a subtle change in channel architecture in the model described in Fig. 13 would produce a channel which necessarily had to open before TEA block could occur as opposed to a channel in which TEA block could occur in either the open or the closed state of the channel.

### Effects of Extracellular Potassium Ions

Armstrong (1971) originally proposed that QA and potassium ions interact within the channel ("knock-off" mechanism) based on observations of the peak outward current elicited by strong depolarizing voltage pulses with a double pulse protocol in both low and high levels of $K_o$. The results in Fig. 12 in this study provide a different view of this hypothesis. The steady state cur-

rent elicited by a strong depolarizing pulse in the presence of QA ions is unaffected by a change in $K_o$, which is consistent with a lack of an interaction between potassium and QA ions within the channel. However, the peak current was reduced by an increase of $K_o$ in a manner which suggests that channel activation rate was reduced. This result is surprising, because channel activation is not affected by an increase in $K_o$ alone (Clay, 1984; Armstrong & Matteson, 1986), nor are channel kinetics altered, directly, by QA ions alone. Rather, the effect on gating appears to require both QA ions in the cellular interior and an increase of potassium ions in the cellular exterior. The mechanism by which such an effect might occur is not obvious. An increase in $K_o$ clearly does have an effect on membrane current waveforms in the presence of QA blockade, as originally demonstrated by Armstrong (1971). However, the interpretation of this result is not straightforward.

### Comparison with Other Preparations

TEA may be the most widely used of all potassium channel blockers, although it generally has been used simply to remove potassium current, especially when applied externally to preparations which have potassium channels with an extracellular TEA receptor (Stanfield, 1983). Relatively few reports concerning the mechanism of blockade at the intracellular receptor have appeared until recent work with cloned potassium channels. The general theme first employed by Armstrong (1969; 1971) of investigating potassium channel structure by using QA ions having various different structures was also used by Coronado and Miller (1982) and Miller (1982) on the sarcoplasmic reticulum $K^+$ channel, and by Villarroel, et al. (1989) on the $Ca^{+2}$ activated $K^+$ channel. Results from the recent $K^+$ channel literature which are most directly relevant to this report and to the work of Armstrong (1969; 1971) are in the study of Choi, et al. (1993) who used the triethylammonium ion derivatives to investigate the intracellular TEA binding site of various mutants of the *Shaker* $K^+$ channel. They concluded that QA ions had two distinct binding sites within the channel, one for the charge on the "head" group of these ions, which is located within the channel, and one for the hydrophobic "tail" located with the putative S6 transmembrane domain of the channel. None of the alterations of the channel obtained by site directed mutagenesis appeared to influence the mechanism of blockade, which is consistent with open channel block for all QA ions, including TEA (*see below*). Consequently, the binding site in the *Shaker* potassium ion channel for the charge on the head group would appear to lie farther away from the intracellular side of the channel than the gate. QA ions may also have two binding sites in the axonal $K^+$ channel as well, but the binding site for the head group would appear to lie closer to the intracellular side of the channel relative to the position of the gating mechanism, as noted above, since TEA blocks via the state independent mechanism.

Perhaps the most compelling evidence in favor of the open channel block model of the *Shaker* $K^+$ channel by intracellular TEA has been provided by Bezanilla, et al. (1991), who found that TEA produces gating charge immobilization in this preparation. Open channel block of RCK2 channels by intracellular TEA has also been reported by Kirsch, Taglialatela, and Brown (1991) based on single channel recordings. In contrast to these results, Taglialatela and Stefani (1993) have shown a lack of gating charge immobilization with TEA for the rat brain potassium channel, DRK1, and Perozo, et al. (1992) have noted a lack of effect of TEA on $I_K$ gating current from squid axons. Consequently, TEA block of the *Shaker* and the RCK2 $K^+$ channels is consistent with the open channel block model, whereas TEA block of DRK1 and squid axon $I_K$ channels is consistent with state independent block. As noted above, a relatively subtle change in channel structure could be sufficient to account for these differences. That is, state independent block might be associated with the binding site for TEA lying only slightly away from the channel gate toward the intracellular side of the channel. Similar differences in the mechanism of blockade amongst different types of channels may also occur with regards to the extracellular TEA binding site. Specifically, Kirsch et al. (1991) reported that the open channel block model is appropriate for the effects of extracellular TEA on the RCK2 channel. In contrast, Wong, Davidson, and Kehl (1994) recently reported that tetrapentylammonium applied extracellularly blocked but did not alter the time constant of tail currents of $K^+$ channels in rat pituitary melanotrophs. This result is consistent with the state independent block model. A similar result was reported by Chow (1991) concerning block of calcium current in squid neurons by $Cd^{+2}$. Indeed, he suggested the state independent block model as a possible mechanism for his results. Consequently, the delayed rectifier potassium ion channel in squid giant axons may not be the only preparation for which the state independent block model is appropriate.

The author gratefully acknowledges Paul Guth of Cambridge Chemical for custom synthesis of the $C_n$ compounds used in this study, Michael Rogawski for helpful discussion of this work, and Adam Sherman of Alembic Software and Vijay Kowtha for technical assistance in data acquisition and analysis.

## References

Armstrong, C.M. 1966. Time course of $TEA^+$-induced anomalous rectification in squid giant axons. *J. Gen. Physiol.* **50**:491–503

Armstrong, C.M. 1969. Inactivation of the potassium conductance and related phenomena caused by quaternary ammonium ion injected in squid axons. *J. Gen Physiol.* **54**:553–575

Armstrong, C.M. 1971. Interaction of tetraethylammonium ion derivatives with the potassium channels of giant axons. *J. Gen. Physiol.* **58:**413–437

Armstrong, C.M. 1975. Potassium pores of nerve and muscle membranes. *In:* Membranes. V3. G. Eisenman, editor. pp. 325–358 Marcel Dekker, New York

Armstrong, C.M. 1990. Potassium channels. Architecture and channel blockers. *In:* Potassium Channels: Basic Function and Therapeutic Aspects. T. Colatsky, editor. pp. 1–15. A.R. Liss, New York

Armstrong, C.M., Binstock, L. 1965. Anomalous rectification in the squid giant axon injected with tetraethylammonium chloride. *J. Gen. Physiol.* **48:**859–872

Armstrong, C.M., Hille, B. 1972. The inner quaternary ammonium ion receptor in potassium channels of the node of Ranvier. *J. Gen. Physiol.* **59:**388–400

Armstrong, C.M., Matteson, D.R. 1986. The role of calcium ions in the closing of K channels. *J. Gen. Physiol.* **87:**817–832

Bezanilla, F., Perozo, E., Papazian, D., Stefani, E., 1991. Molecular basis of gating charge immobilization in *Shaker* potassium channels. *Science* **254:**679–683

Blatz, A.L., Magleby, K.L. 1984. Ion conductance and selectivity of single calcium-activated potassium channels in cultured rat muscle. *J. Gen. Physiol.* **84:**1–23

Choi, K.L., Mossman, C., Aube, J., Yellen, G. 1993. The internal quaternary ammonium receptor site of *Shaker* potassium channels. *Neuron.* **10:**533–541

Chow, R.H. 1991. Cadium block of squid calcium currents. Macroscopic data and a model. *J. Gen. Physiol.* **98:**751–770

Clay, J.R. 1984. Potassium channel kinetics in squid axons with elevated levels of external potassium concentration. *Biophys. J.* **45:**481–485

Clay, J.R. 1985. Comparison of the effects of internal $TEA^+$ and $Cs^+$ on potassium current in squid giant axons. *Biophys. J.* **48:**885–892

Clay, J.R. 1988. Lack of effect of internal fluoride on potassium channels in squid axons. *Biophys. J.* **53:**647–648

Clay, J.R. 1991. A paradox concerning ion permeation of the delayed rectifier potassium ion channel in squid giant axons. *J. Physiol.* **444:**499–511

Clay, J.R. 1992. A re-examination of the mechanism of blockade of the delayed rectifier by $TEA^+$. Must the channel open for blockade to occur? *Biophys. J.* **61:**289a (*Abstr.*)

Clay, J.R., Shlesinger, M.F. 1983. Effects of external cesium and rubidium on outward potassium currents in squid axons. *Biophys. J.* **42:**43–53

Coronado, R., Miller, C. 1982. Conduction and block by organic cations in a $K^+$ selective channel in sarcoplasmic reticulum incorporated into planar lipid bilayers. *J. Gen. Physiol.* **79:**529–547

Fitzhugh, R. 1965. A kinetic model of the conductance change in nerve membrane. *J. Cell. Comp. Physiol.* **66:**111–118

French, R.J., Shoukimas, J.J. 1981. Blockage of squid axon potassium conductance by internal tetra-N-alkylammonium ions of various sizes. *Biophys. J.* **34:**271–291

French, R.J., Wells, J.B. 1977. Sodium ions as blocking agents and charge carriers in the potassium channel of the squid giant axon. *J. Gen. Physiol.* **70:** 707–724

Goldman, D.E. 1943. Potential, impedance, and rectification in membranes. *J. Gen. Physiol.* **27:**37–60

Hartmann, H.A., Kirsch, G.E., Drewe, J.A., Taglialatela, M., Joho, R.H., Brown, A.M. 1991. Exchange of conduction pathways between two related $K^+$ channels. *Science.* **251:**942–944

Hodgkin, A.L., Huxley, A.F. 1952. A quantitative description of membrane current and its application to conduction and excitation in nerve. *J. Physiol.* **117:**500–544

Hodgkin, A.L., Katz, B. 1949. The effect of sodium ions on the electrical activity of the giant axon of the squid. *J. Physiol.* **108:**37–77

Kirsch, G.E., Taglialatela, M., Brown, A.M. 1991. Internal and external TEA block in single cloned $K^+$ channels. *Am. J. Physiol.* **261:**C583–590

Miller, C. 1982. Bis-quaternary ammonium blockers as structural probes of the sarcoplasmic reticulum $K^+$ channel. *J. Gen. Physiol.* **79:**869–892

Perozo, E., Papazian, D.M., Stefani, E., Bezanilla, F. 1992. Gating currents in *Shaker* $K^+$ channels. Implications for activation and inactivation models. *Biophys. J.* **62:**161–171

Stanfield, P.R. 1983. Tetraethylammonium ions and the potassium permeability of excitable cells. *Rev. Physiol. Biochem. Pharmacol.* **97:**1–67

Swenson, R.P., Jr. 1981. Inactivation of potassium current in squid axon by a variety of quaternary ammonium ions. *J. Gen. Physiol.* **77:**255–271

Taglialatela, M., Stefani, E. 1993. Gating currents of the cloned delayed-rectifier $K^+$ channel DRK1. *Proc. Nat. Acad. Sci. USA* **90:**4758–4762

Villarroel, A., Alvarez, O., Oberhauser, A., Latorre, R. 1989. Probing a $Ca^{+2}$ activated $K^+$ channel with quaternary ammonium ions. *Pfluegers Archv.* **413:**118–126

Wong, K., Davidson, J.-I., Kehl, S.J. 1994. Tetrapentylammonium (TPA) blocks the slowly-activating, slowly-inactivating $K^+$ current ($I_K$(s)) of rat pituitary melanotrophs. *Soc. Neurosci Abstr.* **20:**1525

Woodhull, A.M. 1973. Ionic blockade of sodium channels in nerve. *J. Gen. Physiol.* **61:**687–708

Yellen, G., Jurman, M.E., Abramson, T., MacKinnon, R. 1991. Mutations affecting internal TEA blockade identify the probable pore-forming region of a $K^+$ channel. *Science* **251:**939–942